

# Experimental and Numerical Study of Forced Response of Small-Scale Lean-Premixed Pure Hydrogen Flames

Hyebin Kang, Kyu Tae Kim\*

Department of Aerospace Engineering, Korea Advanced Institution of Science and Technology (KAIST)  
Daejeon, 34141, Republic of Korea

## 1 Introduction

Hydrogen is a promising fuel for future power generation as a means of reducing carbon emissions as well as a means of chemical energy storage via hydrolysis from renewable power sources, e.g. solar or wind [1]. The different chemical properties of hydrogen, however, pose significant challenges in existing industrial gas turbine systems mainly designed to operate with natural gas. Hydrogen flame is well-known to have higher flame speed and higher flame temperature, implying that the flame will stabilize differently with a different size or shape, exhibit different combustion dynamics, and also affects combustion performance such as flashback and NO<sub>x</sub> emissions [2].

Extensive studies have been carried out to understand the static and dynamic stabilities of premixed hydrogen flame [3-6]. Compared to conventional methane flames, researchers found that pure hydrogen flames can trigger intense thermoacoustic oscillations coupled to higher acoustic mode even under atmospheric pressure [3,4]. These oscillations can cause immediate damage or shorten hardware life through an increased heat transfer and pressure fluctuations, thus it is of crucial importance to be able to predict and eliminate combustion instabilities.

Typically, low-order network models combined with flame transfer function (FTF) have been used widely for instability studies [7,8]. The flame transfer function, which relates flame response to velocity oscillations, can be obtained directly from experiments [7] or high-fidelity numerical simulations [8]. Here we investigate the forced response of small-scale lean-premixed hydrogen flames to imposed velocity oscillations in both experimental and numerical approaches. We perform LES for premixed hydrogen flames with and without external acoustic forcing, validating calculations with experimental results, and finally gathering insights into the dynamics of forced hydrogen flames.

## 2 Methodology

### Experimental setup

Figure 1(a) shows a schematic diagram of a laboratory-scale combustion test rig that consists of an inlet section, a multi-element nozzle assembly, an optically-accessible quartz tube, and a stainless-steel variable-length combustion section. The fully-premixed H<sub>2</sub>/air mixtures are fed into the inlet plenum

and pass the nozzle assembly consisting of 293 small-scale multi-element injectors (reference) or 37 injectors (reduced), as displayed in Fig. 1(b). Each injector element has an inner diameter of 3 mm and is distributed in a concentric rectangular pattern on a dump plane with a diameter of 142 mm.

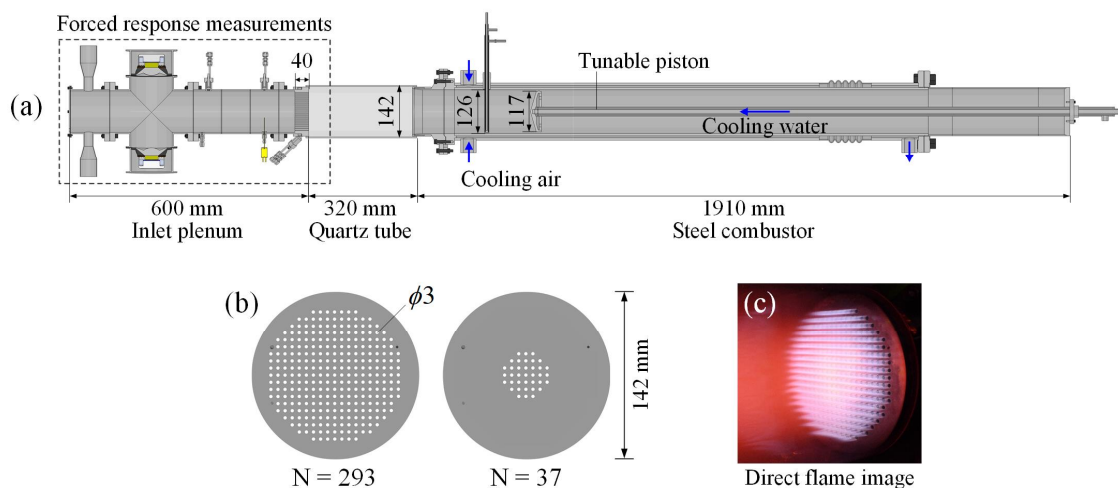


Figure 1: Schematic of laboratory-scale experimental test rig equipped with multi-element nozzle. (a) Cross-sectional view of the test rig. (b) Spatial arrangements of 293 and 37 multi-element injector arrays. (c) Direct flame image of pure hydrogen flame ensemble. All dimensions in mm.

Acoustic oscillations are induced by a pair of two loudspeakers (Morel EW428) located upstream of the burner that can produce harmonic forcing in a wide range of frequencies under high power conditions. A sinusoidal wave generated from an arbitrary function generator (Tektronics, AFG31000) is used for harmonic excitation at selected frequencies. The amplitude of acoustic velocity oscillations is set to approximately 5% of the mean nozzle velocity to capture the linear response of flame.

Hotwire anemometry (HWA), consisting of a constant temperature anemometer system (TSI 1750) and a single normal probe (TSI 1210-10), is used to measure velocity oscillations. The probe is located right upstream of the nozzle element; thus, calibration is carried out using the injector assembly transfer function between the nozzle upstream and downstream velocity oscillations.

Global OH\* chemiluminescence emission intensity is used as an indicator of the flames' global heat release rate. For this measurement, a photomultiplier tube (PMT, Hamamatsu model H7732-10) coupled with a bandpass filter ( $309 \pm 5$  nm) is positioned at  $90^\circ$  with respect to the flow direction. A Princeton Instruments PI-MAX4 ICCD camera, with a UV  $f/4.5$  Nikkor lens and an OH\* bandpass filter centered at 310 nm (10 nm FWHM) is utilized to record the ensemble-averaged flame images.

For the OH-PLIF measurements, a flashlamp-pumped frequency-doubled Nd:YAG laser (Continuum Surelite II-10) is used to pump a tunable dye laser (NarrowScan Radiant Dyes) operating at a repetition rate of 10 Hz. The excited OH fluorescence signal near 310 nm is acquired at  $90^\circ$  using a Princeton Instruments PI-MAX4 ICCD camera ( $1024 \times 1024$  pixel resolution) fitted with a UV  $f/4.5$  Nikkor lens and a bandpass filter (Laser Components, model LC-HBP310/10-50).

In our experiments, the temperature of reactant mixtures and mean nozzle velocity were set to 293 K and 20 m/s, respectively. The equivalence ratio was set to 0.482, equivalent to the adiabatic flame temperature of 1600 K. For the given operating condition, forced measurements were carried out under thermoacoustically stable conditions by adjusting the piston position to exclude the influence of self-excited instabilities.

### Numerical method

The commercial solver Ansys Fluent 2021R1 is used for CFD simulations due to its broad range of well-validated physical modeling capabilities. Based on the laboratory-scale experimental setup, Fig. 2 shows a simplified numerical model consisting of five injector elements with an inner diameter of 3 mm. The length of 200 mm in the combustion chamber is only a fifth of the nozzle length to save computational resources. A sufficiently high length-to-height ratio is still assured.

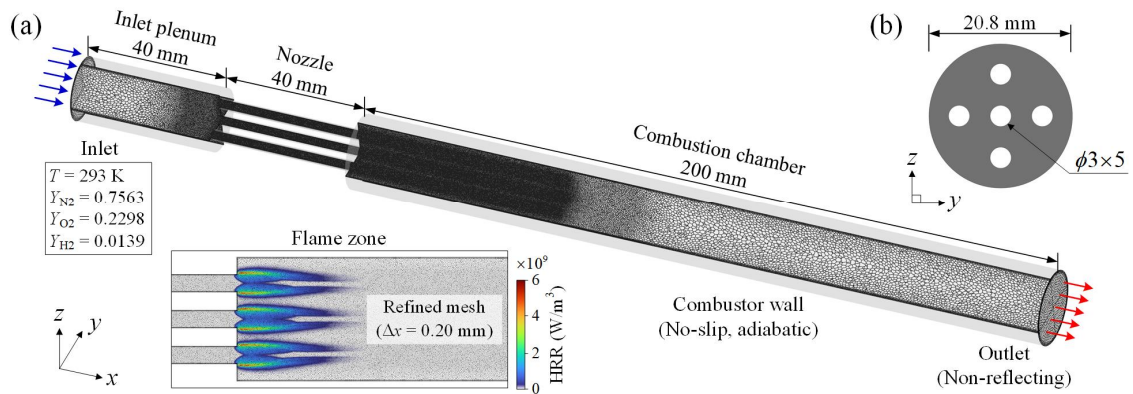


Figure 2: Computational mesh, boundary conditions, and dimensions for 3-D large eddy simulation.

A fully homogeneous mixture of air and fuel enters from the left with a uniform inlet velocity at an initial temperature of 293 K. The mass flow rates of these inlets were calculated through Cantera to produce an equivalence ratio of 0.482, an adiabatic temperature of 1600 K, and a mean nozzle velocity of 20 m/s. No-slip adiabatic walls are imposed at all boundaries. The outlet is modeled with a non-reflecting boundary condition that allows us to neglect non-physical reflections of steady or unsteady flow waves at the far field. A 10-species of combustion mechanism with 19-reactions is introduced to capture hydrogen-air kinetics, further details of this mechanism are provided in [11].

For the LES approach, the 3-D unsteady, compressible, reacting flow equations are discretized with the 2<sup>nd</sup>-order central differencing scheme in order to minimize numerical diffusion. The standard Smagorinsky-Lilly model is applied to capture the sub-grid scale turbulent eddies. For turbulent combustion modeling, the thickened flame model resolving the flame front on the LES grid was applied. While maintaining the correct laminar flame speed, a thickening factor of 5 is applied in the flame region in the present study. The computational grid is approximately 4 million polyhedral elements with a grid resolution of 0.20 mm on the flame location. A time-step of 5  $\mu$ s is used throughout this study. These settings resulted from a grid convergence study ( $\Delta x = 0.30$  mm, 0.25 mm, 0.20 mm, and 0.15 mm) to confirm sufficient spatial and temporal resolution.

Table 1: Summary of methods.

	Experiment	Simulation
Methods	Loudspeaker, Hotwire anemometry (HWA), Photomultiplier tube (PMT), OH* chemiluminescence, OH-PLIF	3D, LES, Smagorinsky-Lilly turbulence model, Thickened flame model ( $F = 5$ ), Ansys Fluent

### 3 Results and discussion

We first measure the flame transfer function of pure hydrogen flame ensemble over a broad range of frequencies ( $f = 60 - 1000$  Hz,  $\Delta f = 20$  Hz). This can be directly measured by imposing small-velocity fluctuations in the upstream flow and monitoring the global heat release rate in the flame with a photomultiplier tube (PMT).

As shown in Fig. 3, the FTF gain exhibits low-pass filter behavior in general. The gain for the 100% H<sub>2</sub> FTF (N293) does not decrease significantly until a much higher frequency compared to 60% H<sub>2</sub> flame with CH<sub>4</sub> (N293). The flame is thus able to continue to amplify oscillations over a much wider frequency range than is possible in a hydrogen-enriched methane combustion system. This further reinforces the early investigations that high-frequency thermoacoustic oscillations cannot be ignored in hydrogen systems [3, 6]. Meanwhile, the FTF phase quasi-linearly decreases with increasing hydrogen concentrations. This behavior is primarily controlled by the overall flame length which decreases with increasing hydrogen concentration.

We also evaluated the effect of nozzle density by comparing the FTF results of 100% H<sub>2</sub> flames between N293 and N37 nozzle arrays (See Fig. 1(b)). The results show similar trends overall with some minor differences, which can be attributed to the fact that significant flame-flame interactions are strongly mitigated in pure hydrogen conditions. Based on this observation, the numerical simulations were performed on a simplified 5-nozzle model.

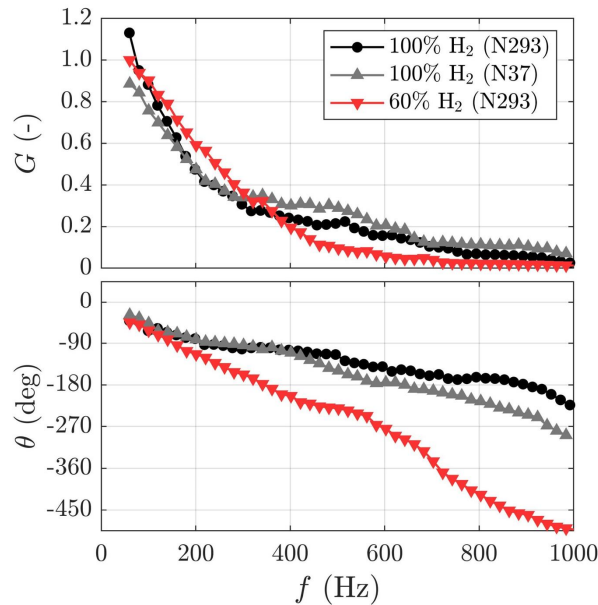


Figure 3: FTF measurements of  $N = 293$  and  $N = 37$  nozzle array.

To verify the simulation, the flame structure was compared with experimental results based on two-dimensional OH\* chemiluminescence and OH-PLIF images. From left to right, Fig. 3 shows contours of H<sub>2</sub> and OH mass fractions, heat release rate from LES in comparison with Abel-deconvoluted OH\* distribution, and OH-PLIF images of center flames. Our results confirm that LES is able to reproduce the flame structure in good agreement with experimental measurements. Note that the flame height of pure hydrogen flame is around  $x/D = 9$  and the heat release rate is stronger at the flame base region while a flame tip can be observed to be open.

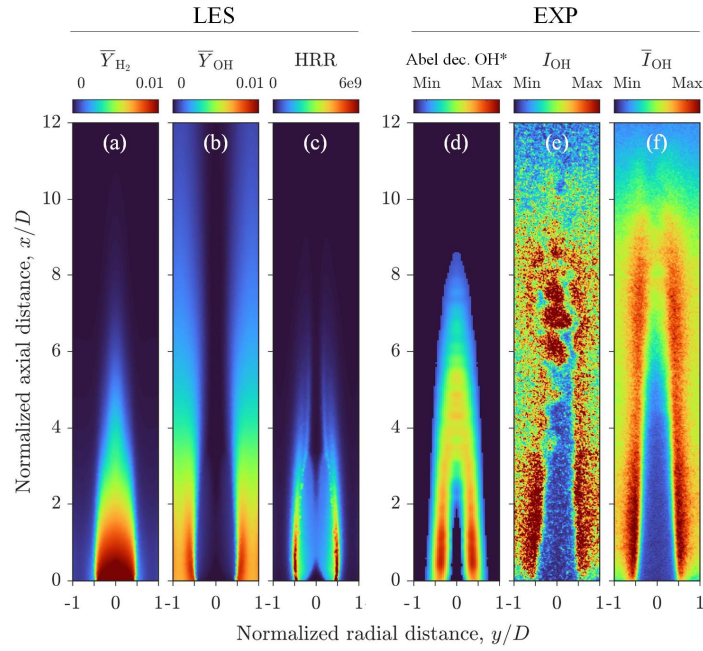


Figure 4: Contours of (a)  $\text{H}_2$  mass fraction, (b) OH mass fraction, (c) heat release rate from LES, compared to (d) Abel-deconvoluted  $\text{OH}^*$  chemiluminescence, (e) instantaneous OH-PLIF, (f) ensemble-averaged OH-PLIF images of center flames from experiments.

To gain a detailed understanding of flame dynamics under imposed velocity oscillations, the sinusoidal form of the perturbation was chosen to imitate the acoustic forcing generated by loudspeakers. The amplitude of the oscillations should be small enough such that the heat release rate perturbations do not experience non-linear effects, while still being observable above the local turbulence. Figure 5 shows the flame behavior at a specific forcing frequency of 600 Hz. It is found that the heat release rate (HRR) distribution from LES is able to reproduce the flame dynamics captured from experiments.

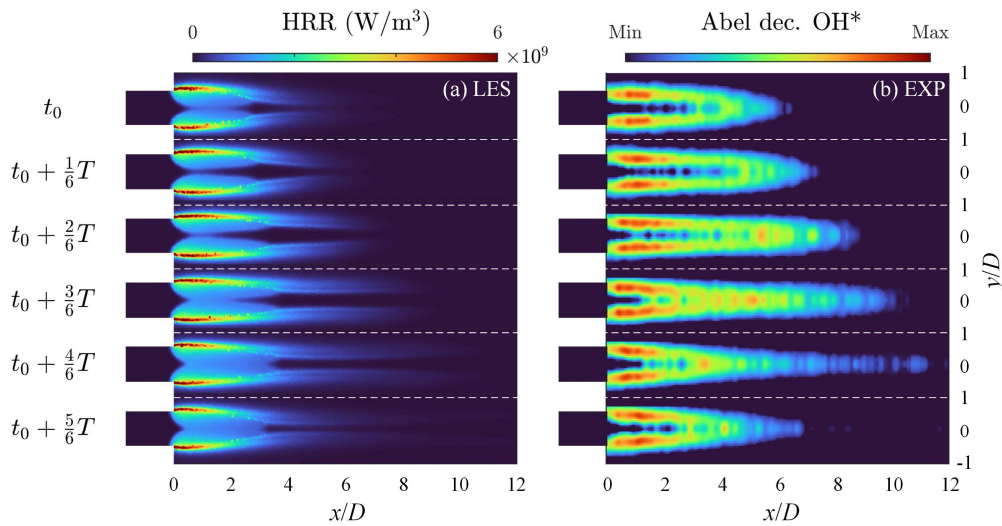


Figure 5: Instantaneous heat release rate from LES (left) and Abel-deconvoluted  $\text{OH}^*$  chemiluminescence images of the center flames (right) over one oscillation cycle at the forcing frequency of 600 Hz.

## 4 Conclusion and remark

The forced response of small-scale lean-premixed hydrogen flames was investigated in both experimental and numerical approaches. The qualitative evaluation of the LES results showed good agreement with the experimental results. In the next step, the system identification (SI) method should be applied to determine the flame transfer function (FTF) over a broad range of frequencies and compared against global experimental data quantitatively.

## Acknowledgments

This work was supported by the Korea Institute of Energy Technology Evaluation and Planning (KETEP) and the Ministry of Trade, Industry & Energy (MOTIE) of the Republic of Korea (Grant # 20206710100060, Development of Low Nox Hydrogen Combustor for Distributed Power Generation Gas Turbine; Grant # 20214000000310, Human Resources Program in Energy Technology).

## References

- [1] Beér JM. (2000). Combustion technology developments in power generation in response to environmental challenges. *Prog. Energy Combust. Sci.* 26: 301.
- [2] Noble D, Wu D, Emerson B, Sheppard S, Lieuwen T, Angello L. (2021). Assessment of current capabilities and near-term availability of hydrogen-fired gas turbines considering a low-carbon future. *ASME. J. Eng. Gas Turbines Power.* 143: 041002.
- [3] Kang H, Lee M, Kim KT. (2022). Measurements of self-excited instabilities and nitrogen oxides emissions in a multi-element lean-premixed hydrogen/methane/air flame ensemble. *Proc. Combust. Inst.* In-press.
- [4] Lee T, Kim KT. (2022). High-frequency transverse combustion instabilities of lean-premixed multislit hydrogen-air flames. *Combust. Flame.* 238: 111899.
- [5] Chterev I, Boxx I. (2021). Effect of hydrogen enrichment on the dynamics of a lean technically premixed elevated pressure flame. *Combust. Flame.* 225: 149.
- [6] Aguilar JG, Æsøy E, Dawson JR. (2022). The influence of hydrogen on the stability of a perfectly premixed combustor. *Combust. Flame.* 245: 112323.
- [7] Kim KT, Lee JG, Quay BD, Santavicca DA. (2010). Spatially distributed flame transfer functions for predicting combustion dynamics in lean premixed gas turbine combustors, *Combust. Flame.* 157: 1718.
- [8] Garcia AM, Bras SL, Prager J, Häringer M, Polifke W. (2022). Large eddy simulation of the dynamics of lean premixed flames using global reaction mechanisms calibrated for CH<sub>4</sub>-H<sub>2</sub> fuel blends. *Phys. Fluids.* 34: 095105
- [9] Ó Conaire M, Curran HJ, Simmie JM, Pitz WJ, Westbrook CK. (2004), A comprehensive modeling study of hydrogen oxidation. *Int. J. Chem. Kinet.* 36: 603.